Received: 9 May 2022 | Revised: 12 June 2022 | Accepted: 14 June 2022

DOI: 10.1111/mpp.13242

Molecular Plant Pathology WILEY

ORIGINAL ARTICLE

Actin-bundling protein fimbrin regulates pathogenicity via organizing F-actin dynamics during appressorium development in *Colletotrichum gloeosporioides*

Yi Zhang[1,2] | Bang An[1,2] | Wenfeng Wang[1] | Bei Zhang[1,2] | Chaozu He[1,2] | Hongli Luo[1,2] | Qiannan Wang[1,2]

[1]Hainan Key Laboratory for Sustainable Utilization of Tropical Bioresource, Key Laboratory of Biotechnology of Salt Tolerant Crops of Hainan Province, College of Tropical Crops, Hainan University, Haikou, China

[2]Sanya Nanfan Research Institute of Hainan University, Hainan Yazhou Bay Seed Laboratory, Sanya, China

Correspondence
Qiannan Wang, Hainan Key Laboratory for Sustainable Utilization of Tropical Bioresource, Key Laboratory of Biotechnology of Salt Tolerant Crops of Hainan Province, College of Tropical Crops, Hainan University, Haikou 570228, Hainan, China.
Email: wangqiannan@hainanu.edu.cn

Funding information
National Natural Science Foundation of China, Grant/Award Number: 32000102 and 32001846; Natural Science Foundation of Hainan Province, Grant/Award Number: 321RC454

Abstract

Anthracnose caused by *Colletotrichum gloeosporioides* leads to serious economic loss to rubber tree yield and other tropical crops. The appressorium, a specialized dome-shaped infection structure, plays a crucial role in the pathogenesis of *C. gloeosporioides*. However, the mechanism of how actin cytoskeleton dynamics regulate appressorium formation and penetration remains poorly defined in *C. gloeosporioides*. In this study, an actin cross-linking protein fimbrin homologue (CgFim1) was identified in *C. gloeosporioides*, and the knockout of *CgFim1* led to impairment in vegetative growth, conidiation, and pathogenicity. We then investigated the roles of CgFim1 in the dynamic organization of the actin cytoskeleton. We observed that actin patches and cables localized at the apical and subapical regions of the hyphal tip, and showed a disc-to-ring dynamic around the pore during appressorium development. CgFim1 showed a similar distribution pattern to the actin cytoskeleton. Moreover, knockout of *CgFim1* affected the polarity of the actin cytoskeleton in the hyphal tip and disrupted the actin dynamics and ring structure formation in the appressorium, which prevented polar growth and appressorium development. The *CgFim1* mutant also interfered with the septin structure formation. This caused defects in pore wall overlay formation, pore contraction, and the extension of the penetration peg. These results reveal the mechanism by which CgFim1 regulates the growth and pathogenicity of *C. gloeosporioides* by organizing the actin cytoskeleton.

KEYWORDS
actin cytoskeleton, appressorium, *Colletotrichum gloeosporioides*, fimbrin, pore, septin

Yi Zhang and Bang An contributed equally to this work.

This is an open access article under the terms of the Creative Commons Attribution-NonCommercial-NoDerivs License, which permits use and distribution in any medium, provided the original work is properly cited, the use is non-commercial and no modifications or adaptations are made.
© 2022 The Authors. *Molecular Plant Pathology* published by British Society for Plant Pathology and John Wiley & Sons Ltd.

1 | INTRODUCTION

The *Colletotrichum* species are a group of pathogenic fungi that infect a wide range of host plants and cause anthracnose diseases worldwide (Dean et al., 2012; O'Connell et al., 2012). Most *Colletotrichum* species use a hemibiotrophic and multistage strategy during the infection life cycle. Elucidating the biology of *Colletotrichum* development and infection processes could provide information for controlling strategies against anthracnose diseases.

In filamentous fungi, the establishment of polarity is important for growth and development. The growth of hyphae in most fungi takes place almost exclusively in the apical zone, and this process is associated with the polarized trafficking of secretory vesicles to the organizing centre called the Spitzenkörper (Spk) (Riquelme, 2013; Riquelme et al., 2018). The Spk is thought to be composed of the cytoskeleton, vesicles, ribosomes, and other undefined components (Riquelme et al., 2018). In addition, a lot of hemibiotrophic fungi, including *Colletotrichum* species, infect the host via a specialized infection cell called an appressorium. To enter plant tissue, a conidium produces a polarized germ tube that grows a short distance and differentiates at its apex to form an appressorium (Wilson & Talbot, 2009). The appressorium synthesizes melanin, glycerol, and other components to generate enormous internal turgor pressure. After maturation and repolarization of the appressorium, an invasive peg emerges from the base of the appressorium and forces through the leaf cuticle.

The cytoskeleton organization plays an important role in the establishment of polarity and cell differentiation in fungi (Takeshita et al., 2014; Xiang & Plamann, 2003). Microfilaments are a dynamic cytoskeleton structure that exists in all eukaryotic cells. Microfilaments are composed of monomeric globular actin (G-actin), linear actin polymers (F-actin), motor proteins, and actin-binding proteins (ABPs) (Berepiki et al., 2011). There are three higher-order F-actin structures found in *Saccharomyces cerevisiae* and *Aspergillus nidulans*: patches, cables, and rings (Araujo-Bazán et al., 2008; Kilmartin & Adams, 1984). Actin patches and cables are usually located at the Spk, serve as tracks for endocytosis and exocytosis, and are involved in hyphal tip growth (Riquelme & Sánchez-León, 2014), whereas actin rings participate in septum and appressorium formation (Dulal et al., 2021; González-Rodríguez et al., 2016; Ryder et al., 2013). In *Colletotrichum graminicola*, the actin cytoskeleton presents as patches and cables in the hyphal tips (Wang & Shaw, 2016), while during septum formation, F-actin contractile rings briefly appear at the base of the septum (Wang & Shaw, 2016). The actin dynamics are precisely controlled by a series of ABPs. For example, *Magnaporthe oryzae* actin-binding protein MoAbp1 functions as a protein scaffold linking actin-regulating kinase MoArk1 and capping protein MoCAP (Li et al., 2019); MoArk1 phosphorylates MoCAP to regulate actin dynamics in hyphae and appressoria (Li et al., 2017; Wang et al., 2013). MoMyo1, a member of the class I myosin proteins, is highly expressed during conidiation and infection, and knockdown mutants exhibit defects in fungal growth, cell wall integrity, endocytosis, and formation of appressorium-like structures (ALS) of *M. oryzae* (Zheng et al., 2021). In *M. oryzae* appressoria, septin is deposited on membranes via association with membrane lipids (He et al., 2020) and interacts with F-actin to form higher-order rings around the appressorium pore (Dagdas et al., 2012; Dulal et al., 2021). Then a narrow penetration peg emerges from the pore and penetrates the rice leaf (Wilson & Talbot, 2009).

In plants, actin-bundling factor proteins play important roles in organizing actin filaments into higher-order structures (Ye et al., 2009). Fimbrins, which were first identified from chicken intestinal microvilli (Bretscher & Weber, 1980), are well-characterized actin-bundling proteins and are widely present in organisms ranging from yeast to mammals. All members of the fimbrin family contain two highly conserved actin-binding domains (ABDs), each including two calponin-homology domains, making it possible to bundle or cross-link two adjacent actin filaments. In *Arabidopsis*, there are five *FIMBRIN* genes (Kovar et al., 2000). Among these fimbrin proteins, FIMBRIN1 and FIMBRIN5 are required for the polarity of actin bundles in pollen tubes and are involved in pollen development (Su et al., 2012; Wu et al., 2010). In fission yeast, only one fimbrin (Sac6) has been identified, and it plays important roles in endocytosis, cytokinesis, and polarization (Christensen et al., 2019; Skau et al., 2011; Skau & Kovar, 2010). In *A. nidulans*, fimbrin assembles as patches and is enriched in the apex of hyphal tips, implying a role in endocytosis (Upadhyay & Shaw, 2008). In *Ashbya gossypii*, AgSAC6, a homologue of fimbrin, is required for fast polarized hyphal growth, polarity maintenance, and endocytosis (Jorde et al., 2011). Research on *M. oryzae* showed that fimbrin accumulates with actin patches at the hyphal subapical collar (Gupta et al., 2015). Moreover, knockout of the fimbrin-coding gene resulted in impaired Spk maintenance and reduced actin bundle formation, preventing the polar growth and pathogenicity of *M. oryzae* (Li et al., 2020). During *M. oryzae* appressorium morphogenesis, the formation of a cortical septin ring is dependent on the appressorium functionality, and the formation of F-actin rings is necessary for the remodelling of septin (Dulal et al., 2021). However, whether fimbrin is involved in the remodelling of these ring structures is still not known. The actin cytoskeleton dynamics and the biological functions of fimbrin of *C. gloeosporioides*, one of the most notorious phytopathogens, also remain unknown.

In this study, we generated a *C. gloeosporioides fimbrin* (*CgFim1*) knockout mutant, labelled the actin cytoskeleton and septin structure using Lifeact-GFP and CgSeptin4-GFP respectively, and performed live-cell imaging to reveal the architecture and dynamics of the F-actin and septin networks during hyphal tip growth and appressorium morphogenesis. Our results showed that CgFim1 is necessary for the polar assembly of F-actin patches and cables in hyphal tips and the F-actin ring around the appressorial pore, which are necessary for hyphal growth, conidiation, and pathogenesis. In addition, CgFim1 is involved in the F-actin-mediated septin remodelling and the formation of the pore wall overlay in the appressorium. Our findings extend the understanding of how fimbrin regulates the pathogenesis of fungal pathogens and the functions of the actin cytoskeleton in *C. gloeosporioides*.

2 | RESULTS

2.1 | Generation of *fimbrin* mutant strains

The bioinformation of fimbrins and their roles in the growth and development of *C. gloeosporioides* have not been elucidated. Through a BLAST search, one *fimbrin* gene, *CgFim1*, was identified in the *C. gloeosporioides* genome. *CgFim1* contains a 1938 bp open reading frame separated by four introns, and it encodes a protein of 645 amino acids (Figure S1a). The domain analysis revealed that CgFim1 contains two EF-hand-like motifs at the N-terminus, and four Calponin homology domains, which are also known as the actin-binding domain 1 (ABD1) and actin-binding domain 2 (ABD2). In addition, the phylogenetic analysis showed that fimbrins are highly conserved in plant-pathogenic fungi (Figure S1b). To investigate the physiological roles of CgFim1, the *CgFim1* gene was knocked out via the split-marker recombination strategy in *C. gloeosporioides* (Figure S2). In addition, the knockout mutant Δ*CgFim1* was complemented by introducing a *CgFim1* expression cassette driven by its native promoter, and the complementation mutant was named Res-Δ*CgFim1* (Figure S3a).

2.2 | CgFim1 plays important roles in vegetative growth, stress tolerance, and conidiation

When cultured on solidified minimal medium, the colony growth of Δ*CgFim1* was significantly reduced compared to the wild type (WT) and Res-Δ*CgFim1*, with the colony diameter decreasing 22% and 35% at 3 and 5 days postinoculation, respectively. In addition, the colonies of Δ*CgFim1* were irregular circles with ragged growing edges, compared with the regular circular colonies of the WT (Figure 1a,b). The stress tolerance of the strains was investigated by incubation on medium supplemented with various chemicals. The results showed that the sensitivity of Δ*CgFim1* to sorbitol and Congo red was significantly reduced in comparison to that of the WT and Res-Δ*CgFim1*, and the sensitivity to iprodione was slightly increased, whereas for the other chemicals Δ*CgFim1* showed similar sensitivity to the WT and Res-Δ*CgFim1* (Figure 1a,c). A conidiation assay was then conducted. The results showed that the conidiation of Δ*CgFim1* was drastically decreased, with the conidial yield only about 2% of that of the WT (Figure 1e). Moreover, the Δ*CgFim1* conidia were smaller than that of WT and Res-Δ*CgFim1* strains, with decreases in both conidial length and width (Figure 1d,f). These results suggest impairment in the development and conidiation of Δ*CgFim1*.

2.3 | CgFim1 is required for full pathogenicity

We next analysed the pathogenicity of the strains on intact or prewounded rubber tree leaves. When droplets of the conidial suspensions (2×10^5 conidia/ml, 5 μl) were inoculated on the prewounded leaves, Δ*CgFim1* caused smaller lesions than the WT and Res-Δ*CgFim1*, although all the strains infected leaves with a disease incidence of 100% (Figure 2a–c). On the intact leaves, the disease incidence caused by Δ*CgFim1* was only 33%, compared with 87% and 83% for WT and Res-Δ*CgFim1*. Moreover, Δ*CgFim1* induced a smaller lesion on intact leaves in comparison with the WT and Res-Δ*CgFim1* (Figure 2d–f). These results indicate that CgFim1 plays an important role in pathogenicity of *C. gloeosporioides* and especially in the initial penetration process to plant tissues.

2.4 | CgFim1 plays crucial roles in appressorium formation and invasive hyphae development

We then analysed appressorium formation and invasion hyphae development by incubation of *C. gloeosporioides* conidia on polystyrene plates and onion epidermis. After incubation on plates for 12 h, over 80% of the conidia of WT and Res-Δ*CgFim1* strains produced short germ tubes and differentiated to form appressoria, whereas for Δ*CgFim1* only 6% of the conidia formed appressoria. After 24 h, appressoria of WT and Res-Δ*CgFim1* strains were melanized. In comparison, only 21% of Δ*CgFim1* conidia formed appressoria with relatively longer germ tubes (Figure 3a,c). To further validate the reduction in virulence of Δ*CgFim1*, we performed a penetration assay using onion epidermis. Most of the appressoria of WT and Res-Δ*CgFim1* strains developed invasive hyphae (also called primary hyphae) that penetrated the onion cells after incubation for 24 h. Although Δ*CgFim1* formed long germ tubes growing on the surface of the onion, only a few conidia formed appressoria and invasive hyphae (Figure 3b,d). In summary, the appressorium formation rate and penetration of the onion epidermis of Δ*CgFim1* were markedly affected, indicating that CgFim1 regulates full virulence in *C. gloeosporioides*.

2.5 | CgFim1 plays a role in the actin cytoskeleton in the polarized hyphal tip and appressorium

To investigate the role of CgFim1 in actin organization, we first examined the actin structure in conidia and the hyphal tip of *C. gloeosporioides*. In conidia, Lifeact-EGFP-labelled actin patches and cables were uniformly distributed in the conidial cytoplasm, but the mean fluorescence intensity of Δ*CgFim1* was lower than that of the WT (Figure 4a,b). In growing WT vegetative hyphae, actin cables and patches accumulated in the apical and subapical regions, suggesting a link with hyphal tip growth, whereas in Δ*CgFim1* hyphal tips, a concomitant decrease in the amount and a reduced polarity of F-actin were detected (Figure 4c,d). These data suggest that the actin patches are relatively uniformly dispersed in Δ*CgFim1* conidia and hyphal tips.

Given that the actin organization in the appressorium of *C. gloeosporioides* is not well understood, we simultaneously imaged the actin cytoskeleton during appressorium development (Figures S4 and 4e). In the early stage, as shown in Figure S4, obvious actin cables

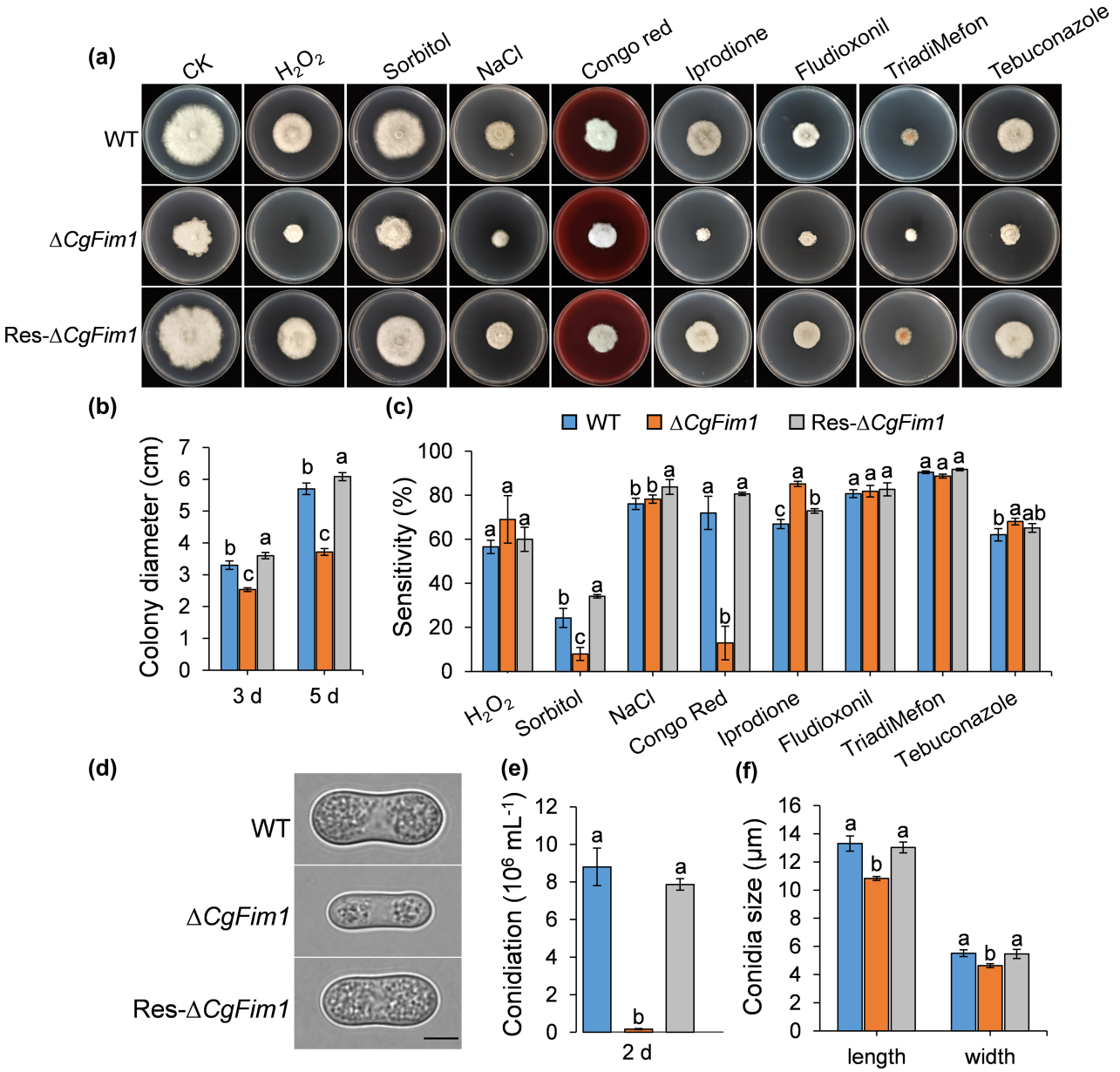

FIGURE 1 Colony growth and conidiation assays. (a) Colony morphology of wild type (WT), Δ*CgFim1*, and complemented strain (Res-Δ*CgFim1*) incubated on minimal medium supplemented with different chemicals for 5 days. CK, control check. (b) Colony diameter of the strains on minimal medium after 3 and 5 days. (c) Quantitative analysis of chemical sensitivity after incubation for 5 days. The sensitivity was calculated by comparing the colony area with that of CK. (d) Conidial morphology. Scale bar = 5 μm. (e) Conidiation of the strains. (f) Conidial size of the strains. Values are shown as the mean ± standard deviation (*SD*) of three samples. Columns with different letters indicate significant differences ($p < 0.05$)

and patches formed in the apical zone of an elongating germ tube (0.5–1.5 h) during germination. As the tip of the germ tube swelled to form an appressorium (3 h), the actin cytoskeleton organized into a ring structure at the base of the appressorium (also called the septation site). Subsequently, the actin cytoskeleton reassembled in a disc structure in the centre of the appressorium (4.5 h). Images in Figure 4e show that in the WT, once the appressorium formed, the F-actin disc contracted along with the appressorial pore during appressorium development and reorganized to form a toroidal structure around the pore after the appressorium matured (Figure 4e, upper panels). In Δ*CgFim1*, the appressorium formation was delayed, F-actin discs and rings failed to form, and instead actin patches were mainly dispersed in appressoria with low fluorescence intensity (Figure 4e, lower panels). We conclude that CgFim1 is required for actin organization during hyphal tip growth and appressorium formation of *C. gloeosporioides*.

2.6 | CgFim1 is involved in the regulation of septin dynamics

In *M. oryzae*, the septins are also organized into a ring structure in the appressorium (Dagdas et al., 2012). To examine the role of

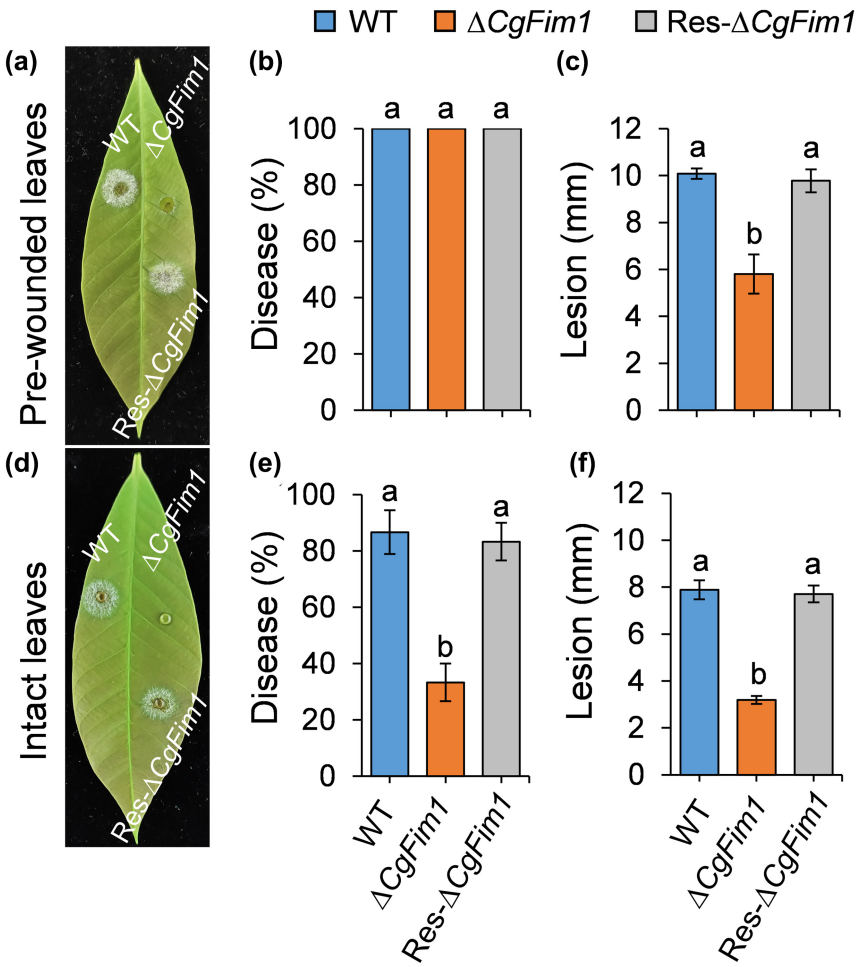

FIGURE 2 Pathogenicity assay on rubber tree leaves. (a) Disease symptoms of wild type (WT), Δ*CgFim1*, and complemented strain (Res-Δ*CgFim1*) on prewounded leaves at 3 days postinoculation (dpi). (b) Disease incidence of the strains on prewounded leaves after 3 dpi. (c) Mean lesion diameters on prewounded leaves at 3 dpi. (d) Disease symptoms of the strains on intact leaves at 3 dpi. (e) Disease incidence of the strains on intact leaves after 3 dpi. (f) Mean lesion diameters on intact leaves at 3 dpi. Values are shown as the mean ± standard deviation (*SD*) of three groups of samples. Columns with different letters indicate significant differences ($p < 0.05$)

CgFim1 in the septin dynamics, we first carried out live-cell imaging of Septin4 (CgSep4) during appressorium maturation by expressing CgSep4-GFP in *C. gloeosporioides* (Figure 5a). The result revealed that CgSep4 initially formed a disc then gradually contracted to form a small ring around the pore in *C. gloeosporioides*. However, knockout of *CgFim1* delayed septin disc formation along with the inhibition of appressorium development. Moreover, the knockout of *CgFim1* completely prevented normal septin ring formation (Figure 5a).

In *M. oryzae*, the septin ring provides cortical rigidity during pressure production and serves as a diffusion barrier to organize polarity at the appressorium base (Dagdas et al., 2012; Ryder et al., 2013, 2019). We set out to investigate appressorial collapse in response to osmotic pressure produced by polyethylene glycol (PEG). The collapse assay showed that appressorial collapse of the WT strain increased in a dose-dependent manner. When PEG 8000 at a concentration of 50% was used, the collapse rate of Δ*CgFim1* was about 59% (Figure 5b,c); in comparison, the collapse rate of the WT strain was only 9%. This result shows that the cortical rigidity of appressoria was significantly decreased in Δ*CgFim1*, suggesting that CgFim1 contributes to appressorium turgor generation.

2.7 | CgFim1 shows a similar distribution pattern to the actin cytoskeleton

To investigate the dynamics of CgFim1 distribution, we labelled CgFim1 with green fluorescent protein (GFP) (Figure S3). CgFim1-GFP patches were uniformly distributed in conidia and there was a polarized pattern in vegetative hyphal tips (Figure S5a). During appressorial development, CgFim1 was initially localized in discrete puncta of the cytoplasm and at the periphery of the appressoria (2 h). These were then recruited to the cytoplasm around the pore (4 h), contracted (6 h), and formed a ring structure surrounding the pore (8–24 h) (Figure S5b). The dynamics of CgFim1 distribution appears analogous to that of the actin structures, revealing the important role of CgFim1 in the organization of the actin cytoskeleton.

2.8 | CgFim1 is required for the formation of the appressorial pore and penetration peg

As targeted deletion of *CgFim1* prevented the formation of either the F-actin or septin networks around the appressorial pore, we deduced that the appressorial pore might also be affected in Δ*CgFim1*.

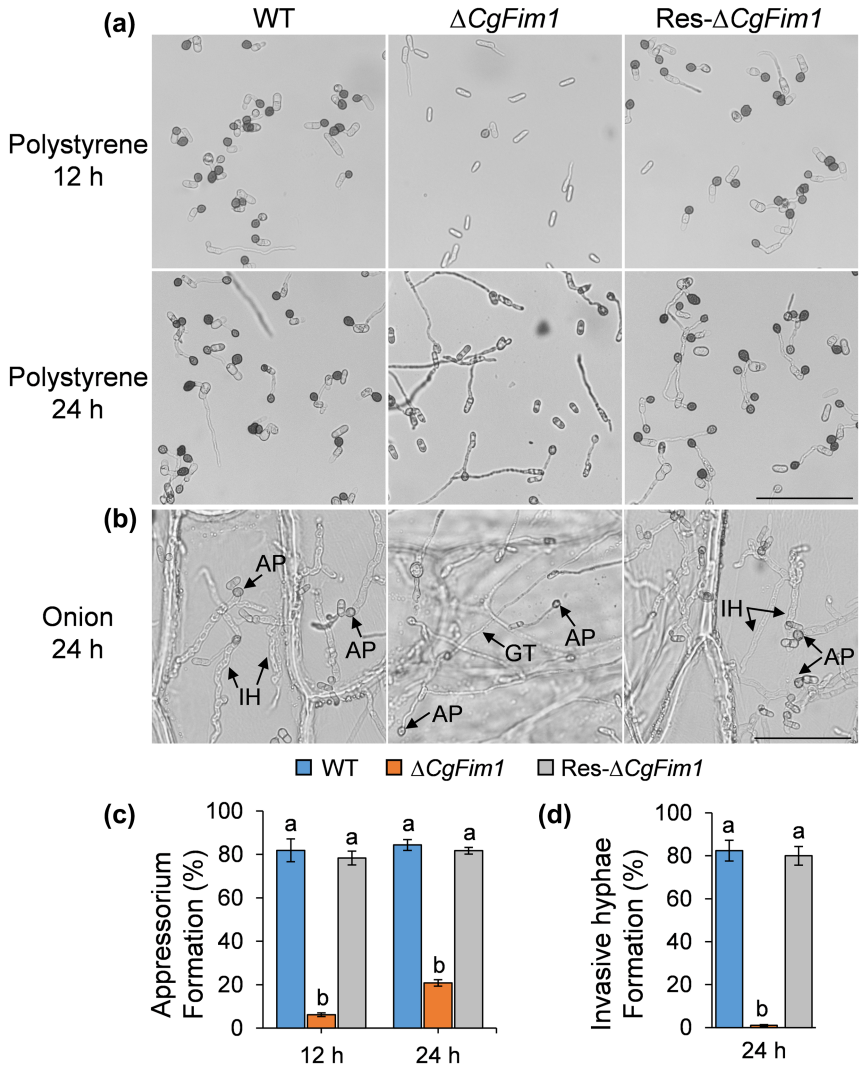

FIGURE 3 Appressorium formation on hydrophobic polystyrene plates and onion epidermis. (a) Appressorium formation of wild type (WT), Δ*CgFim1*, and complemented (Res-Δ*CgFim1*) strains after incubation on hydrophobic plates for 12 and 24 h. Scale bar = 50 μm. (b) Appressorium formation and penetration of the strains after incubation on onion epidermis for 24 h. AP, appressorium; GT, germ tube; IH, invasive hypha. Scale bar = 50 μm. (c) The appressorium formation rate of the strains on hydrophobic polystyrene plates. (d) The invasive hyphae formation rate of the strains after incubation on onion epidermis for 24 h. Values are shown as the mean ± standard deviation (*SD*) of three groups of samples, and each group of samples comprises 100 conidia. Columns with different letters indicate significant differences ($p < 0.05$)

To test this hypothesis, we analysed the appressorium using a scanning electron microscope (Figure 6a). After incubation for 24 h on hydrophobic plastic surfaces and destruction of the appressoria using a cell scraper, the cell bases of appressoria were examined. The images show that in the WT strain there was a typical pore located in the centre of the appressorium bottom, and the pore was surrounded by a specialized garland-like structure called the pore wall overlay (Figure 6a). In addition, an obvious indentation was found in the pore, indicating the formation of a penetration peg. In Δ*CgFim1*, the pore wall overlay disappeared in 94.2% of the appressoria, and pores were undented (Figure 6a,b). Moreover, quantitative analysis revealed that the pores produced by Δ*CgFim1* were larger than those produced by the WT strain (Figure 6c). We concluded that CgFim1 is required for appressorial pore integrity and penetration peg formation. In *M. oryzae*, the invasive peg emerges from the appressorial pore and inserts into a plant cell (Howard et al., 1991). To test whether the aberrant appressorial pore and the absence of pore wall overlay are related to the impairment of invasive hyphae in Δ*CgFim1*, the germination behaviour on onion epidermis was investigated. The results showed that the invasive hyphae emerged from the appressorial pore, which was colocalized with the septin ring (Figure 7b). However, we did not observe an F-actin toroidal network in the appressorium, suggesting that there might be a remodelling of the actin cytoskeleton during invasive hyphae development (Figure 7a). Knockout of *CgFim1* led to the interference of appressorium formation, deformed ring structures, and loss of invasive hyphae. Taken together, these results suggest that the failure in penetration and host cell colonization of Δ*CgFim1* is due to its defects in appressorial pore development.

2.9 | CgFim1-mediated toroidal F-actin networks are required for septin remodelling

In *M. oryzae*, the appressorial septin disc formation is driven by actin ring contraction (Dulal et al., 2021). To test whether the CgFim1-mediated actin dynamics are involved in the process, we first quantitatively assessed the response of Δ*CgFim1* appressorium formation to actin-depolymerizing agent latrunculin A (LatA) and the actin filament polymerizing and stabilizing drug jasplakinolide (Jasp). After incubation on hydrophobic plastic surfaces for 2 h, we treated *C. gloeosporioides* conidia with LatA or Jasp for another 10 h. The

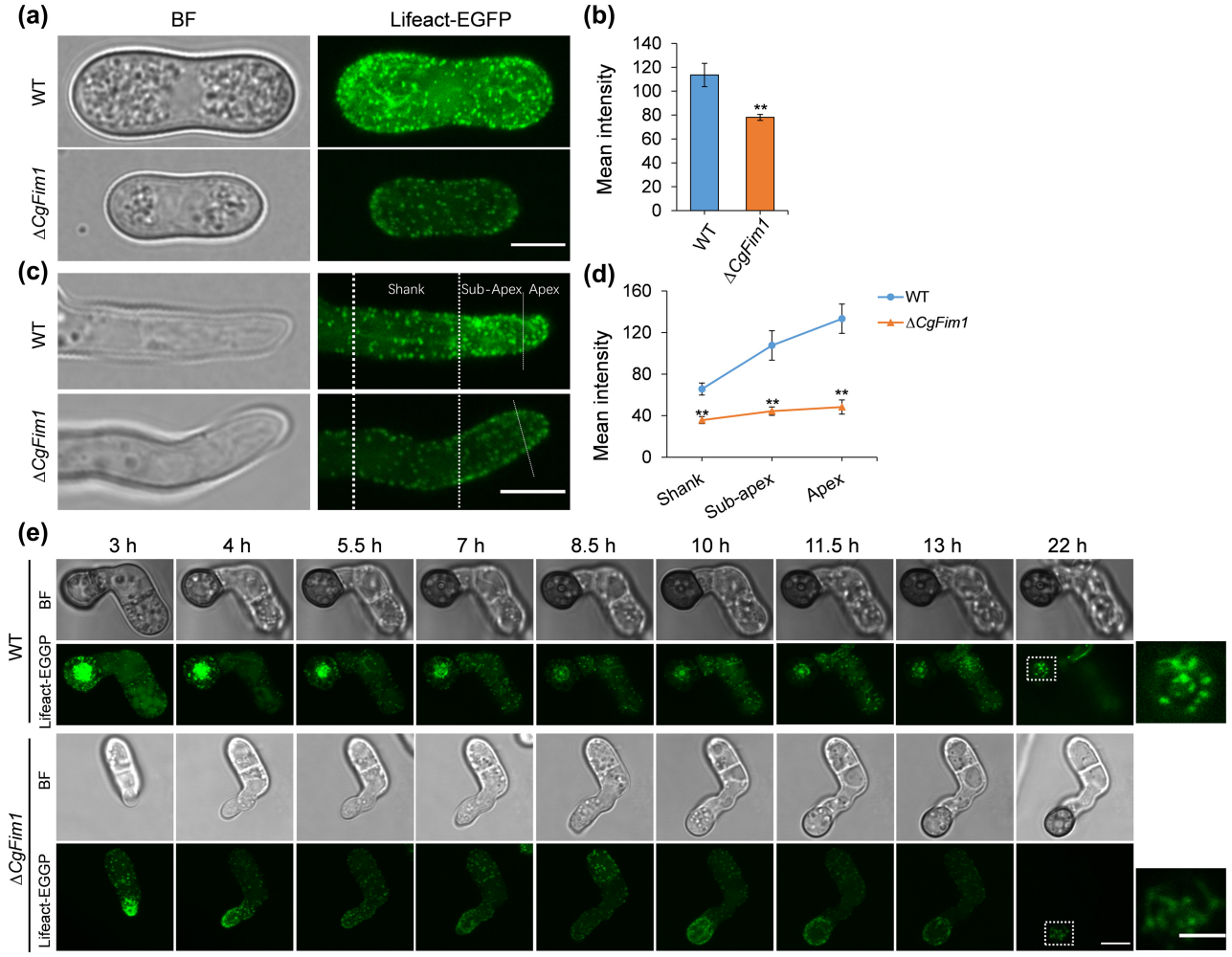

FIGURE 4 CgFim1 regulates the actin cytoskeleton in the conidia, hyphal tips, and appressoria of *Colletotrichum gloeosporioides*. Actin was labelled by expressing Lifeact-EGFP in the strains. (a) Actin cytoskeleton in conidia of the wild type (WT) and Δ*CgFim1* strains. Scale bar = 5 μm. (b) The mean fluorescence intensity of the actin cytoskeleton in conidia of the strains. (c) Actin cytoskeleton in the hyphal tips of the strains. The hyphal tip is divided into three zones by white dotted lines: apex, subapex, and shank. Scale bar = 5 μm. (d) Graph showing mean fluorescence intensity of the actin cytoskeleton in the apex, subapex, and shank of hyphal tips. At least 10 hyphae were measured for each strain. Values are shown as the mean ± standard deviation (*SD*) of the samples. Asterisks indicate significant differences at $p < 0.01$ (**). (e) Time-lapse sequences comparing the localization and dynamics of the actin cytoskeleton in the appressoria of the strains. Scale bar = 5 μm. Images in the white dashed boxes are enlarged and presented in the rightmost column; scale bar = 2 μm

results showed that both 0.1 and 1 μM LatA treatment significantly affected the formation of appressoria in the WT strain. However, only 1 μM LatA showed a slight inhibition effect on the appressorium formation in Δ*CgFim1* (Figure 8a). For the Jasp treatment, appressorium formation in the WT was insensitive to Jasp, but for Δ*CgFim1*, Jasp sightly increased appressorium formation (Figure 8b). We then investigated the effect of LatA and Jasp on the F-actin and septin networks in the appressoria. The actin cytoskeleton in WT appressoria became punctate after exposure to LatA for 22 h, similar to the distribution pattern in the nontreated Δ*CgFim1* appressoria. The septin ring was also significantly disrupted by LatA treatment (Figure 8c,e,f), whereas in Δ*CgFim1* appressoria, LatA treatment resulted in a further disruption of the actin cytoskeleton. In line with our expectations, exposure to Jasp increased the F-actin polymerization and the percentage of toroidal F-actin networks compared with the control (Figure 8d–f). Collectively, these results suggest that CgFim1-mediated toroidal F-actin networks are required for septin remodelling.

3 | DISCUSSION

Actin-bundling proteins are a group of factors that function in organizing actin filaments into higher-order structures. Among these ABPs, fimbrins are well-characterized in vertebrates, plants, and several fungi. However, despite the finding that fimbrins play roles in vegetative growth, polarized tip growth, endocytosis, and pathogenicity in *A. nidulans*, *A. gossypii*, and *M. oryzae* (Jorde et al., 2011; Li et al., 2020; Upadhyay & Shaw, 2008), our understanding of how fimbrins regulate appressorium development and pathogenicity is limited.

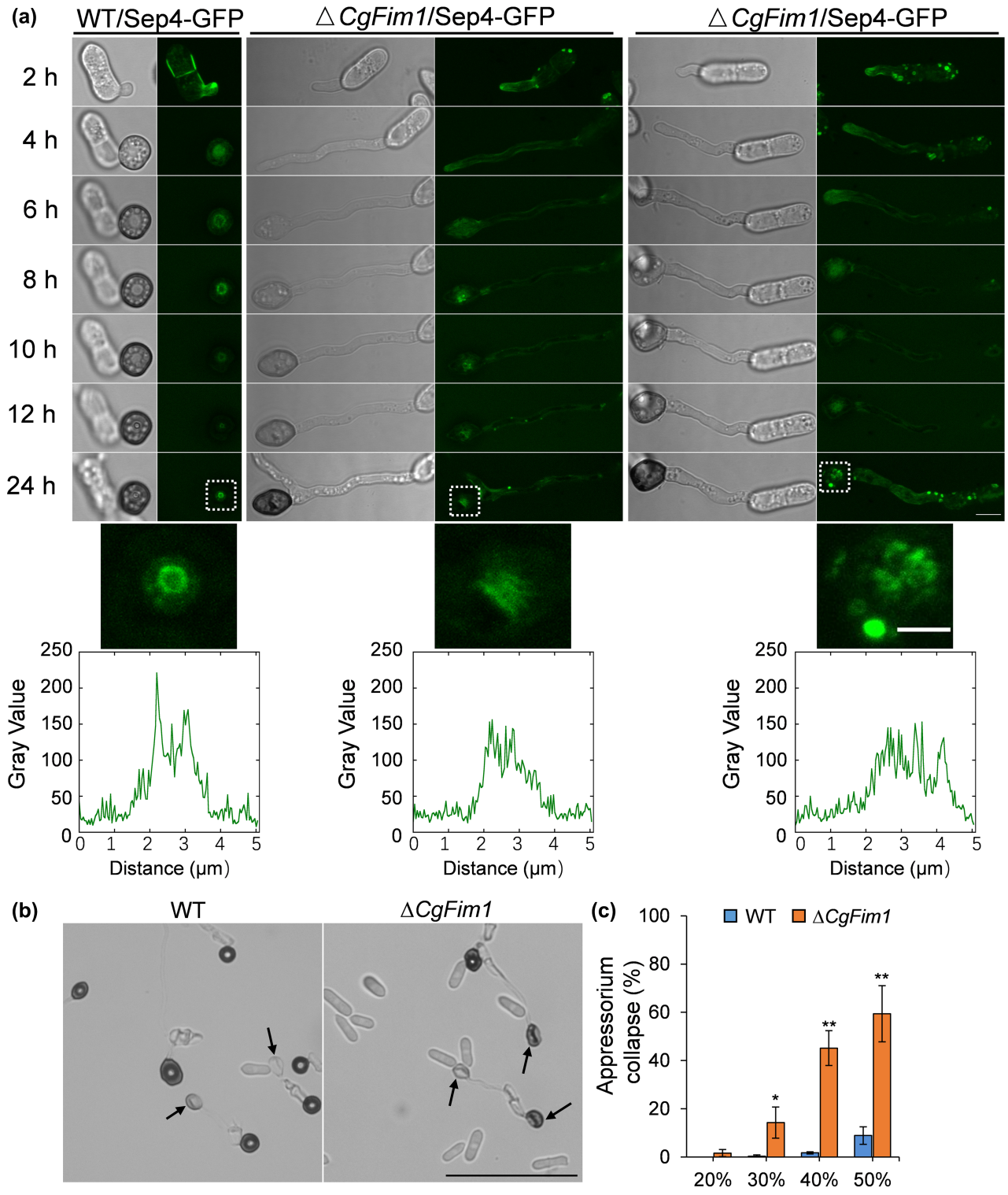

FIGURE 5 CgFim1 is required for the septin dynamics and turgor generation. (a) Time-lapse sequences comparing the localization and dynamics of septin structure in the appressoria of the wild type (WT) and Δ*CgFim1* strains. The septin structure was imaged by expressing CgSep4-GFP. Scale bar = 5 μm. Images in the white dashed boxes are enlarged and presented in the middle panel; scale bar = 2 μm. Line-scan graphs show fluorescence intensity in a horizontal section through an individual appressorium. (b) Appressorium collapse assay of WT and Δ*CgFim1* strains treated with 50% polyethylene glycol (PEG) 8000. The arrows indicate collapsed appressoria. Scale bar = 50 μm. (c) The appressorial collapse rate of WT and Δ*CgFim1* strains after treatment with different concentrations of PEG 8000. Values are shown as the mean ± standard deviation (*SD*) of three groups of samples, and each group comprises 50 conidia. Asterisks indicate significant differences at $p < 0.05$ (*) and $p < 0.01$ (**)

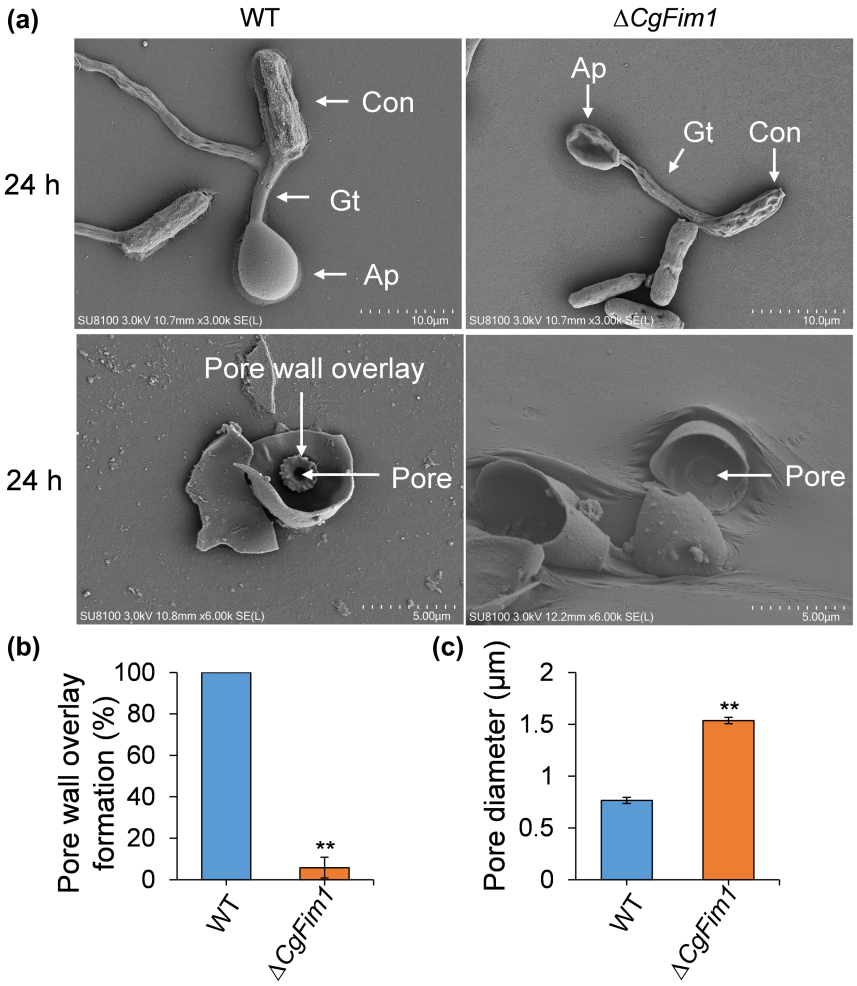

FIGURE 6 CgFim1 is required for the formation of the appressorial pore wall overlay and contraction of the appressorial pore. (a) Scanning electron microscopy images of wild type (WT) and Δ*CgFim1* appressoria after incubation on hydrophobic surfaces for 24 h, without (upper panel) or with (lower panel) scraping to reveal the cell basal structures. Con, conidium; Gt, germ tube; AP, appressorium. Scale bar (upper panel) = 10 μm. Scale bar (lower panel) = 5 μm. (b) The percentage of pore wall overlay formation in WT and Δ*CgFim1* appressoria. (c) The pore diameter in WT and Δ*CgFim1* appressoria. Values are shown as the mean ± standard deviation (*SD*) of three groups of samples, and each group comprises 10 appressoria. Asterisks indicate significant differences at $p < 0.01$ (**)

In addition, the actin organization and dynamics in *C. gloeosporioides* are still unknown. To address this issue, we have performed a comprehensive analysis of the roles of fimbrin in actin dynamics during polarized tip growth and appressorium development. First, a highly conserved fimbrin homologue CgFim1 was identified in *C. gloeosporioides*. To investigate the roles of CgFim1, we then generated a *CgFim1* knockout mutant and investigated the changes in growth and conidiation. Consistent with findings in *A. gossypii* and *M. oryzae* (Jorde et al., 2011; Li et al., 2020), knockout of *CgFim1* severely impaired colony growth of *C. gloeosporioides* (Figure 1a–c). Moreover, ΔCgFim1 produced smaller conidia than the WT, together with a significant impairment in conidial yield (Figure 1d–f). In *M. oryzae*, knockout of *MoFim1* completely inhibited spore production (Li et al., 2020). A pathogenicity assay showed that Δ*CgFim1* was severely affected in pathogenicity. In addition, when inoculated with Δ*CgFim1*, up to 67% of the unwounded leaves did not show disease symptoms (Figure 2), suggesting that the infection ability of Δ*CgFim1* was significantly affected. To cause disease, many phytopathogenic fungi develop appressoria to breach the outer layers of their plant hosts (Talbot, 2019). We therefore speculated that CgFim1 might play a vital role in appressorium development. In the follow-up experiment, we did find that appressorium and invasive hyphae development were seriously affected in Δ*CgFim1* (Figure 3). A similar phenomenon was also observed in the *MoABP1* (actin-binding protein 1) mutant of *M. oryzae*, in which appressorium penetration and invasive growth were disturbed (Li et al., 2019) and knockdown of *MoFim1* led to defective appressoria, of which only a few could invade the rice epidermal sheath cells (Li et al., 2020). These results suggest that fimbrins probably have similar roles in phytopathogenic filamentous fungi in growth, conidiation, and pathogenicity.

Hyphal tip growth and appressorium development are vital for the infection life cycle of filamentous fungi. During the two processes, there is a strong cellular polarity that is precisely regulated by the actin cytoskeleton dynamics (Berepiki et al., 2011; Xiang & Plamann, 2003). The monomeric globular actin first assembles into linear actin polymers called F-actin, then the F-actin is organized into patches, cables, and rings by a series of actin-binding proteins including fimbrins (Berepiki et al., 2011). In *Neurospora crassa*, *A. nidulans*, and *M. oryzae*, the actin patches and cables usually concentrate at apical or subapical regions that are within the core of the Spk in hyphal tips (Delgado-Álvarez et al., 2010; Li et al., 2020; Schultzhaus et al., 2016). Lifeact has been widely used to label F-actin in eukaryotic cells (Li et al., 2020; Riedl et al., 2008; Schumacher, 2012). To visualize the F-actin dynamics of *C. gloeosporioides*, we labelled it with Lifeact-EGFP (Liu, Liu, & Wang, 2021). The live-cell imaging revealed that there was a polarity of cables and patches located at the apical and subapical regions in

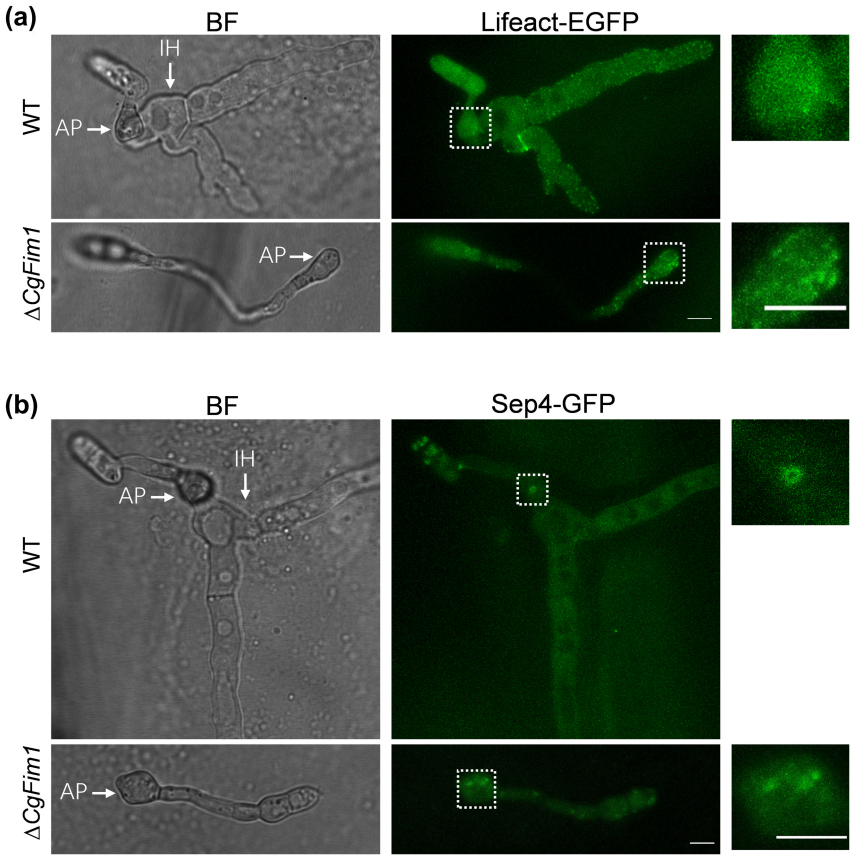

FIGURE 7 CgFim1 regulates actin cytoskeleton and septin organization during appressorium and invasive hyphae development. (a) Micrographs of actin organization in appressoria and invasive hyphae of wild type (WT) and Δ*CgFim1* strains on onion epidermis. AP, appressorium; IH, invasive hypha. Scale bar = 5 μm. (b) Micrographs of septin organization in appressoria and invasive hyphae on onion epidermis. Scale bar = 5 μm. Images in the white dashed boxes in (a) and (b) are enlarged and presented in the rightmost column; scale bar = 5 μm

the hyphal tip of the WT strain, contrasting with ΔCgFim1 in which patches with lower fluorescence intensity were uniformly distributed in conidia and hyphal tips (Figure 4a–d). Similar results were observed in the fimbrin mutants of *A. gossypii* and *M. oryzae* (Jorde et al., 2011; Li et al., 2020), of which the actin distribution and cables at the Spk were affected, thereby leading to impaired hyphal tip growth. These findings proved that CgFim1 is involved in hyphal tip growth by organizing the actin cytoskeleton in *C. gloeosporioides*.

During the appressorium development of *M. oryzae*, the actin cytoskeleton undergoes a precisely regulated dynamic. In the initial stage, F-actin assembles at the appressorium neck after septation, and then depolymerizes and reorganizes into a ring at the base of the appressorial pore (Dulal et al., 2021; Saunders et al., 2010). Mutation of *MoAbp1* causes the mislocalization of F-actin structures in over half of appressoria (Li et al., 2019). *C. graminicola* shows a similar F-actin dynamic during appressorium development to that of *M. oryzae*: the actin cytoskeleton first assembles in cables and patches in elongating germ tubes, then reorganizes into a ring at the septation site, and finally condenses into a circular area at the appressorial pore (Wang & Shaw, 2016). In *C. gloeosporioides*, however, we observed a slightly different pattern of actin dynamic. In the beginning, the actin cables and patches accumulated as a disc in the centre of the appressorium after septation, then the disc reconfigured gradually into a ring (Figures S4 and 4e). In the appressorium of ΔCgFim1, actin patches were uniformly distributed and there was no ring structure formed (Figure 4e). In the appressoria of *M. oryzae* there are no actin discs formed and the F-actin is directly recruited into a ring structure after the contraction of the septin disc (Dulal et al., 2021). Additionally, in comparison with *M. oryzae*, the actin cytoskeleton in *C. graminicola* and *C. gloeosporioides* appressoria needed less time to start reorganization after septation and could not directly assemble into the ring structure (*M. oryzae* 3.5–4 h, *C. graminicola* and *C. gloeosporioides* 1.5–2 h) (Dulal et al., 2021; Wang & Shaw, 2016). These results suggest a difference in actin dynamics of different phytopathogenic fungi. In hyphae of *A. nidulans*, FimA-GFP-labelled patches were concentrated near the hyphal tips, but a patch-depleted zone was found in the apex of growing hyphae (Upadhyay & Shaw, 2008). In *M. oryzae*, fimbrin is localized in the subapical collar region in growing hyphae (Gupta et al., 2015; Li et al., 2020). In this study in *C. gloeosporioides*, CgFim1 assembled in patches and mainly concentrated at both the apical and subapical collar regions of hyphal tips (Figure S5). During appressorium development in *M. oryzae*, MoFim1-GFP also follows a remodelling pattern of periphery–disc–pore surrounding. It should be noted that this pore-surrounding localization of MoFim1 is not a ring structure, but instead fills the entire appressorium except for the pore (Galhano et al., 2017). In our study, CgFim1 structures in the appressorium followed the periphery–aggregation–ring pattern (Figure S5). There was also a remarkable resemblance between the CgFim1-GFP ring and the actin ring structure in the mature appressorium of *C. gloeosporioides*. These results together indicate the important role of CgFim1 in the configuration of the actin cytoskeleton during appressorium formation.

Septins are a broadly conserved family of small morphogenetic guanosine triphosphatases (GTPases). During appressorium formation, septin GTPases form a ring structure that acts as a lateral diffusion barrier

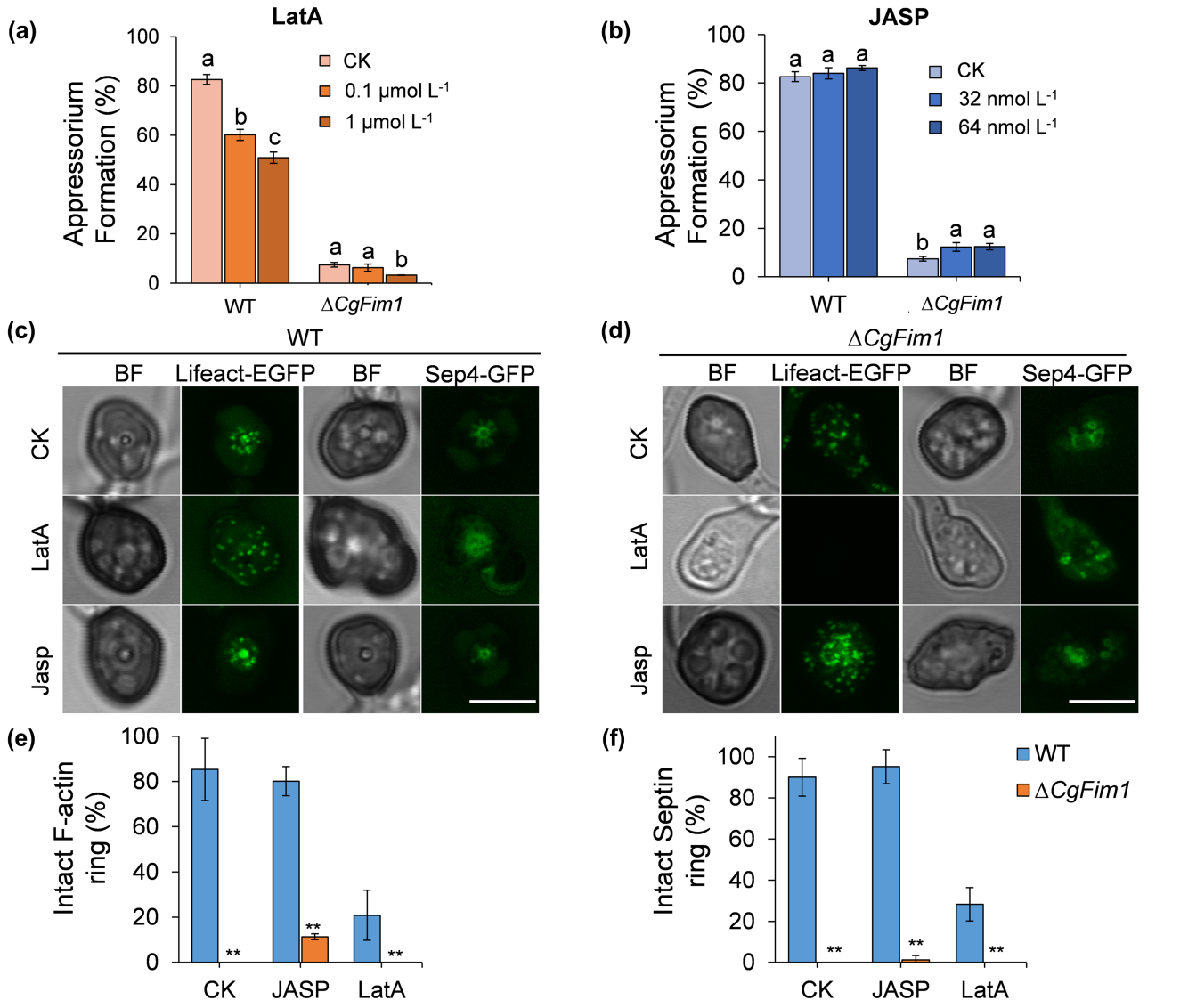

FIGURE 8 CgFim1-mediated actin ring is required for septin remodelling. (a) The appressorium formation rate of wild type (WT) and Δ*CgFim1* strains after treatment with latrunculin A (LatA). (b) The appressorial formation rate after treatment with jasplakinolide (Jasp). Values are shown as the mean ± standard deviation (*SD*) of three groups of samples, and each group comprises 100 conidia. Columns with different letters indicate significant differences ($p < 0.05$). (c) F-actin and septin organization in WT appressoria after treatment with 1 μM LatA or 32 nM Jasp. Scale bar = 5 μm. (d) F-actin and septin organization in Δ*CgFim1* appressoria after treatment with LatA or Jasp. Scale bar = 5 μm. (e) The F-actin ring formation rate in appressoria after treatment with 1 μM LatA or 32 nM Jasp. (f) The septin ring formation rate in appressoria after treatment with LatA or Jasp. Values are shown as the mean ± standard deviation (*SD*) of three groups of samples, and each group comprises 10 appressoria. Asterisks indicate significant differences at $p < 0.01$ (**)

and participates in the re-orientation of the actin cytoskeleton (Dagdas et al., 2012; Saunders et al., 2010). In *M. oryzae*, the mutants *MoSeptin3*, *MoSeptin4*, *MoSeptin5*, and *MoSeptin6* are all affected in F-actin organization (Dagdas et al., 2012). In *Colletotrichum* spp., the roles of septins have not been reported previously. Here we constructed a CgSep4-GFP-expressing strain and visualized the septin structures during appressorium development. Imaging revealed that CgSep4-GFP first forms a disc structure and then gradually contracts to a ring around the appressorial pore in *C. gloeosporioides* (Figure 5a). This pattern of disc-to-ring transition is similar to that in *M. oryzae* (Dulal et al., 2021). In Δ*CgFim1* appressoria, although an incipient septin disc-shaped structure could form, the remodelling from a disc to a ring was impaired (Figure 5a). Unsurprisingly, CgSep4-GFP was also mislocalized and could not form the ring structure in the appressoria of Δ*CgFim1* on onion epidermis (Figure 7b). In *M. oryzae*, LatA-mediated disruption of F-actin leads to fragmented septin structures (Dulal et al., 2021). Consistent with this finding, exposure to LatA also affected the configuration of the septin ring in *C. gloeosporioides* (Figure 8c). We therefore hypothesized that the promotion of the polymerization and stabilization of F-actin may rescue the F-actin and septin ring structures to some extent. As expected, treatment with Jasp enhanced the appressorium formation rate and proportion of intact F-actin ring in Δ*CgFim1* (Figure 8b,d,e). However, Jasp treatment did not alleviate the defective septin structure (Figure 8f). Based on our data, we conclude that CgFim1 is essential for the remodelling of septin.

During the maturation of appressoria, a new wall material that is continuous with the penetrating hyphal cell wall deposits around the appressorial pore, referred to as the pore wall overlay (Bourett & Howard, 1990). This was clearly revealed by transmission electron microscopy of in planta appressoria in *Colletotrichum higginsianum* (Kleemann et al., 2012). However, the internal structure of appressoria of *Colletotrichum* spp. by scanning electron microscopy (SEM) has not been reported previously. Here our SEM results revealed a distinct garland-like structure overlaid around the pore in the appressorium (Figure 6a). In *Oidium neolycopersici* and *Blumeria graminis*, similar garland-like structures have also been found around the appressorial pores and are called O-rings (Jones et al., 2001; Zhang et al., 2005). The O-ring was originally believed to be located outside at the bottom of fungal appressorium pore to effectively seal the host surface (Howard & Ferrari, 1989). However, our study showed that the garland-like structure was inside the appressorium, and also in *O. neolycopersici* and *B. graminis*. Combining all these results, we would rather call this structure the pore wall overlay. What is remarkable is that in *M. oryzae* the pore wall overlay forms at 24–31 h postinoculation and before the emergence of a penetration peg, but no similar garland-like structure was observed by SEM (Bourett & Howard, 1990; Howard et al., 1991; Rocha et al., 2020). Intriguingly, we found that knockout of *CgFim1* led to the disappearance of the pore wall overlay in most of the appressoria in *C. gloeosporioides* (Figure 6a). It has been reported that the pore wall overlay of *C. higginsianum* contains β-1,3-glucan, the most abundant fungal cell wall polysaccharide (Kleemann et al., 2012). Because fimbrins are related to endocytosis in *A. nidulans*, *A. gossypii*, and *M. oryzae* (Jorde et al., 2011; Li et al., 2020; Upadhyay & Shaw, 2008), we speculated that CgFim1 regulates the pore wall overlay formation by controlling the deposition of cell wall material. Additionally, in Δ*CgFim1*, the appressorium pore size was apparently larger than in the WT, and penetration peg indentations were rarely found in the pore (Figure 6a). This is consistent with the low invasive rate of the mutant to onion epidermis (Figure 3). These findings suggest that CgFim1 is crucial for the formation of the pore wall overlay, pore contraction, and the emergence of the penetration peg, and thus for penetration into the host.

Taken together, we propose that CgFim1 is involved in the regulation of the actin cytoskeleton in the hypha and appressorium, and this CgFim1-mediated F-actin interacts with septin to regulate appressorium development in *C. gloeosporioides*. Additionally, CgFim1 is also required for the formation of the pore wall overlay, pore contraction, and the extension of a penetration peg.

4 | EXPERIMENTAL PROCEDURES

4.1 | Characterization and phylogenetic analysis of CgFimbrin1

To identify fimbrin proteins in *C. gloeosporioides* from *Hevea brasiliensis* (BioSample: SAMN17266943, https://www.ncbi.nlm.nih.gov/biosample/17266943), the amino acid sequence of *S. cerevisiae* fimbrin (NP_010414.3) was used to search against the genome of *C. gloeosporioides*. The identified *C. gloeosporioides* fimbrin protein was named CgFimbrin1, and its coding gene was named *CgFim1*. Conserved domains in CgFim1 were searched for using SMART (Letunic et al., 2021). The phylogenetic relationship of CgFim1 with orthologs from other filamentous fungi was analysed through the construction of a maximum-likelihood tree using MEGA 11 (Tamura et al., 2021) with 1000 bootstraps.

4.2 | Generation of mutant strains

CgFim1 was knocked out using a split-marker recombination strategy as shown in Figure S2a according to our previous work (Gao et al., 2022). Three independent knockout mutants were randomly selected and tested for vegetative growth, conidiation, and pathogenicity; as the three mutants showed similar phenotypes, only one mutant was selected for the gene complementation and the following analysis.

The *CgFim1* knockout mutant was complemented by introducing a *CgFim1* expression cassette, which comprised the *CgFim1* sequence together with its native promoter, the terminator of tryptophan synthase of *A. nidulans* (TtrpC), and the hygromycin phosphotransferase gene (*HPT*) (Figure S3a). The Lifeact-EGFP-expressing strain, reported in our previous work, was used as the recipient strain, and *CgFim1* was knocked out as described above (Liu, Liu, & Wang, 2021).

The CgFim1-GFP and CgSep4-GFP strains were constructed via a homologous recombination strategy as shown in Figure S3c. The primers used are listed in Table S1.

4.3 | Vegetative growth, stress tolerance, and conidiation assay

Vegetative growth of *C. gloeosporioides* was examined by culturing the strains on minimal medium. The stress tolerance of the strains was estimated according to our previous work (Liu, Wang, et al., 2021). The chemicals 10 and 50 mM H_2O_2, 0.7 M NaCl, 1 M sorbitol, 0.25 mg/L Congo red, 0.1 μg/ml fludioxonil, 10 μg/ml iprodione, 0.2 μg/ml tebuconazole, and 2.5 μg/ml TriadiMefon were used to simulate stresses. Each treatment contained three replicates, and all experiments were performed twice. The conidiation capacity in the liquid culture of the strains was evaluated, and conidial size was measured with ImageJ software (http://rsbweb.nih.gov/ij/, v. 1.47 g).

4.4 | Pathogenicity assay

The pathogenicity assay was carried out as described in our previous report (Gao et al., 2022). The rubber leaves were divided into two groups, one of intact leaves and the other of prewounded leaves. Then conidial suspensions of strains (5 μl, 2×10^5 conidia/ml^{-1}) were inoculated onto these two groups of leaves to investigate the difference in pathogenicity. Each treatment contained three replicates of 10 leaves, and the entire experiment was repeated three times.

4.5 | Appressorium formation and penetration ability assay

Appressorium formation and the following invasion assay were performed by incubation of *C. gloeosporioides* on hydrophobic plastic plates and onion epidermis, respectively, as described in our previous report (Gao et al., 2022). The relative formation rates were calculated based on data of three replicates, with each replicate comprising 200 conidia.

4.6 | Appressorium collapse assay

C. gloeosporioides conidia were first incubated on hydrophobic plastic plates for 24 h, then PEG 8000 solution at concentrations of 20%, 30%, 40%, and 50% (wt/vol) was dropped onto the appressorium. After incubation for 15 min, the appressorial collapse was observed and the collapse rate was calculated.

4.7 | Fluorescence microscopy

For the visualization of actin or fimbrin structures in hyphae, conidial suspensions of strains expressing Lifeact-EGFP or CgFim1-GFP (5×10^5 conidia/ml) were incubated on YCS-coated glass slides in a moist chamber at 28°C for 4 h. Then the F-actin and fimbrin structures in conidia and the tips of germinated hyphae were captured using a laser scanning confocal microscope (TCS SP8; Leica), with excitation of 488 nm by an argon laser, and an emission wavelength range of 505–525 nm. The hyphal tips were divided into three regions: apex (2 μm, 0–2 μm from the tip), subapex (5 μm, 2–7 μm from the tip), and shank (8 μm, 7–15 μm from the tip) (Cheung et al., 2010), and the fluorescence intensity in the corresponding zones was analysed. For each strain, more than 10 hyphae were measured in each experiment and the entire experiment was conducted twice.

To investigate the fluorescent fusion proteins in the appressorium, conidial suspensions (2×10^5 conidia/ml) were incubated on hydrophobic borosilicate glass coverslips (Thermo Fisher) for 24 h before observation. For timecourse experiments of appressorium development, conidial suspensions (2×10^5 conidia/ml) were cultured in multiwell Labtek chambers (Thermo Fisher) and observed at each time point using a TCS SP8 confocal microscope. All microscopy images were analysed using ImageJ software.

4.8 | Pharmacological treatment of the microfilament cytoskeleton

The effects of LatA (Sigma-Aldrich) and Jasp (Sigma-Aldrich) on the formation of appressoria were investigated by adding the chemicals into conidial suspensions (5×10^5 conidia/ml) at 2 hours postinoculation (hpi). The controls were treated with 0.04% dimethyl sulfoxide (DMSO; Sigma-Aldrich). Appressorium formation was imaged at 12 hpi. This experiment was repeated three times. To analyse the influence of LatA and Jasp on the F-actin and septin ring structures in the appressoria, conidial suspensions (2×10^5 conidia/ml) were cultured in multiwell Labtek chambers, drugs were added at 2 hpi, and observations were made at 24 hpi. DMSO (0.04%) was used as the control treatment.

4.9 | SEM analysis

Appressoria were formed on hydrophobic plastic plates for 24 h. Cell scrapers were used to remove the top half of the appressoria, exposing the bottom of the appressorium that adhered to the plates. After fixing in 2.5% glutaraldehyde and 1% osmium tetroxide successively, all the samples were dehydrated by a series of decreasing concentrations of ethanol and isoamyl acetate. Samples that were attached firmly to the conductive carbon film double-sided tape were sprayed with gold on an ion sputterer sample table, and images were captured with a scanning electron microscope (SU8100; Hitachi).

4.10 | Statistical analysis

Statistical significance analyses were performed using PASW Statistics (IBM). Data with a single variable were analysed by one-way analysis of variance, and mean separations were performed by Duncan's multiple range test. Differences at $p<0.05$ were considered significant.

AUTHOR CONTRIBUTIONS

Q.N.W. and B.A. designed the study. Y.Z., W.F.W., B.Z., and B.A. performed the experiments. Q.N.W. and B.A. wrote the manuscript. H.L.L. and C.Z.H. revised the manuscript. All authors contributed to the article and approved the submitted version.

ACKNOWLEDGEMENTS

This research was funded by the Natural Science Foundation of Hainan Province (321RC454) and the National Natural Science Foundation of China (32001846, 32000102).

CONFLICT OF INTEREST

The authors declare that the research was conducted in the absence of any commercial or financial relationships that could be construed as a potential conflict of interest.

DATA AVAILABILITY STATEMENT

The data that support the findings of this study are available from the corresponding author upon reasonable request.

ORCID

Qiannan Wang https://orcid.org/0000-0001-9059-7717

REFERENCES

Araujo-Bazán, L., Peñalva, M.A. & Espeso, E.A. (2008) Preferential localization of the endocytic internalization machinery to hyphal tips underlies polarization of the actin cytoskeleton in *Aspergillus nidulans*. *Molecular Microbiology*, 67, 891–905.

Berepiki, A., Lichius, A. & Read, N.D. (2011) Actin organization and dynamics in filamentous fungi. *Nature Reviews Microbiology*, 9, 876–887.

Bourett, T.M. & Howard, R.J. (1990) In vitro development of penetration structures in the rice blast fungus *Magnaporthe grisea*. *Canadian Journal of Botany*, 68, 329–342.

Bretscher, A. & Weber, K. (1980) Fimbrin, a new microfilament-associated protein present in microvilli and other cell surface structures. *The Journal of Cell Biology*, 86, 335–340.

Cheung, A.Y., Niroomand, S., Zou, Y. & Wu, H.M. (2010) A transmembrane formin nucleates subapical actin assembly and controls tip-focused growth in pollen tubes. *Proceedings of the National Academy of Sciences of the United States of America*, 107, 16390–16395.

Christensen, J.R., Homa, K.E., Morganthaler, A.N., Brown, R.R., Suarez, C., Harker, A.J. et al. (2019) Cooperation between tropomyosin and α-actinin inhibits fimbrin association with actin filament networks in fission yeast. *eLife*, 8, e47279.

Dagdas, Y.F., Yoshino, K., Dagdas, G., Ryder, L.S., Bielska, E., Steinberg, G. et al. (2012) Septin-mediated plant cell invasion by the rice blast fungus, *Magnaporthe oryzae*. *Science*, 336, 1590–1595.

Dean, R., Van Kan, J.A., Pretorius, Z.A., Hammond-Kosack, K.E., Di Pietro, A., Spanu, P.D. et al. (2012) The top 10 fungal pathogens in molecular plant pathology. *Molecular Plant Pathology*, 13, 414–430.

Delgado-Álvarez, D.L., Callejas-Negrete, O.A., Gómez, N., Freitag, M., Roberson, R.W., Smith, L.G. et al. (2010) Visualization of F-actin localization and dynamics with live cell markers in *Neurospora crassa*. *Fungal Genetics and Biology*, 47, 573–586.

Dulal, N., Rogers, A.M., Proko, R., Bieger, B.D., Liyanage, R., Krishnamurthi, V.R. et al. (2021) Turgor-dependent and coronin-mediated F-actin dynamics drive septin disc-to-ring remodeling in the blast fungus *Magnaporthe oryzae*. *Journal of Cell Science*, 134, jcs251298.

Galhano, R., Illana, A., Ryder, L.S., Rodriguez-Romero, J., Demuez, M., Badaruddin, M. et al. (2017) Tpc1 is an important $Zn(II)_2Cys_6$ transcriptional regulator required for polarized growth and virulence in the rice blast fungus. *PLoS Pathogens*, 13, e1006516.

Gao, X., Wang, Q., Feng, Q., Zhang, B., He, C., Luo, H. et al. (2022) Heat shock transcription factor CgHSF1 is required for melanin biosynthesis, appressorium formation, and pathogenicity in *Colletotrichum gloeosporioides*. *Journal of Fungi*, 8, 175.

González-Rodríguez, V.E., Garrido, C., Cantoral, J.M. & Schumacher, J. (2016) The F-actin capping protein is required for hyphal growth and full virulence but is dispensable for septum formation in *Botrytis cinerea*. *Fungal Biology*, 120, 1225–1235.

Gupta, Y.K., Dagdas, Y.F., Martinez-Rocha, A.L., Kershaw, M.J., Littlejohn, G.R., Ryder, L.S. et al. (2015) Septin-dependent assembly of the exocyst is essential for plant infection by *Magnaporthe oryzae*. *The Plant Cell*, 27, 3277–3289.

He, M., Su, J., Xu, Y., Chen, J., Chern, M., Lei, M. et al. (2020) Discovery of broad-spectrum fungicides that block septin-dependent infection processes of pathogenic fungi. *Nature Microbiology*, 5, 1565–1575.

Howard, R.J., Bourett, T.M. & Ferrari, M.A. (1991) Infection by *Magnaporthe*: an in vitro analysis. In: Mendgen, K. & Lesemann, D.E. (Eds.) *Electron microscopy of plant pathogens*. Berlin: Springer-Verlag, pp. 251–264.

Howard, R.J. & Ferrari, M.A. (1989) Role of melanin in appressorium function. *Experimental Mycology*, 13, 403–418.

Jones, H., Whipps, J.M. & Gurr, S.J. (2001) The tomato powdery mildew fungus *Oidium neolycopersici*. *Molecular Plant Pathology*, 2, 303–309.

Jorde, S., Walther, A. & Wendland, J. (2011) The *Ashbya gossypii* fimbrin SAC6 is required for fast polarized hyphal tip growth and endocytosis. *Microbiological Research*, 166, 137–145.

Kilmartin, J.V. & Adams, A.E. (1984) Structural rearrangements of tubulin and actin during the cell cycle of the yeast *Saccharomyces*. *The Journal of Cell Biology*, 98, 922–933.

Kleemann, J., Rincon-Rivera, L.J., Takahara, H., Neumann, U., van Themaat, E.V.L., van der Does, H.C. et al. (2012) Sequential delivery of host-induced virulence effectors by appressoria and intracellular hyphae of the phytopathogen *Colletotrichum higginsianum*. *PLoS Pathogens*, 8, e1002643.

Kovar, D.R., Staiger, C.J., Weaver, E.A. & McCurdy, D.W. (2000) AtFim1 is an actin filament crosslinking protein from *Arabidopsis thaliana*. *The Plant Journal*, 24, 625–636.

Letunic, I., Khedkar, S. & Bork, P. (2021) SMART: recent updates, new developments and status in 2020. *Nucleic Acids Research*, 49, D458–D460.

Li, L., Chen, X., Zhang, S., Yang, J., Chen, D., Liu, M. et al. (2017) MoCAP proteins regulated by MoArk1-mediated phosphorylation coordinate endocytosis and actin dynamics to govern development and virulence of *Magnaporthe oryzae*. *PLoS Genetics*, 13, e1006814.

Li, Y.-B., Xu, R., Liu, C., Shen, N., Han, L.-B. & Tang, D. (2020) *Magnaporthe oryzae* fimbrin organizes actin networks in the hyphal tip during polar growth and pathogenesis. *PLoS Pathogens*, 16, e1008437.

Li, L., Zhang, S., Liu, X., Yu, R., Li, X., Liu, M. et al. (2019) *Magnaporthe oryzae* Abp1, a MoArk1 kinase-interacting actin binding protein, links actin cytoskeleton regulation to growth, endocytosis, and pathogenesis. *Molecular Plant-Microbe Interactions*, 32, 437–451.

Liu, N., Liu, S.K. & Wang, Q.N. (2021) Construction of a strain with fluorescence labeling of cytoskeleton in *Colletotrichum gloeosporioides*. *Biotechnology Bulletin*, 37, 284.

Liu, N., Wang, Q.N., He, C.Z. & An, B. (2021) CgMFS1, a major facilitator superfamily transporter, is required for sugar transport, oxidative stress resistance, and pathogenicity of *Colletotrichum gloeosporioides* from *Hevea brasiliensis*. *Current Issues in Molecular Biology*, 43, 1548–1557.

O'Connell, R.J., Thon, M.R., Hacquard, S., Amyotte, S.G., Kleemann, J., Torres, M.F. et al. (2012) Lifestyle transitions in plant pathogenic *Colletotrichum* fungi deciphered by genome and transcriptome analyses. *Nature Genetics*, 44, 1060–1065.

Riedl, J., Crevenna, A.H., Kessenbrock, K., Yu, J.H., Neukirchen, D., Bista, M. et al. (2008) Lifeact: a versatile marker to visualize F-actin. *Nature Methods*, 5, 605–607.

Riquelme, M. (2013) Tip growth in filamentous fungi: a road trip to the apex. *Annual Review of Microbiology*, 67, 587–609.

Riquelme, M., Aguirre, J., Bartnicki-García, S., Braus, G.H., Feldbrügge, M., Fleig, U. et al. (2018) Fungal morphogenesis, from the polarized growth of hyphae to complex reproduction and infection structures. *Microbiology and Molecular Biology Reviews*, 82, e00068-17.

Riquelme, M. & Sánchez-León, E. (2014) The Spitzenkörper: a choreographer of fungal growth and morphogenesis. *Current Opinion in Microbiology*, 20, 27–33.

Rocha, R.O., Elowsky, C., Pham, N.T. & Wilson, R.A. (2020) Spermine-mediated tight sealing of the *Magnaporthe oryzae* appressorial pore–rice leaf surface interface. *Nature Microbiology*, 5, 1472–1480.

Ryder, L.S., Dagdas, Y.F., Kershaw, M.J., Venkataraman, C., Madzvamuse, A., Yan, X. et al. (2019) A sensor kinase controls turgor-driven plant infection by the rice blast fungus. *Nature*, 574, 423–427.

Ryder, L.S., Dagdas, Y.F., Mentlak, T.A., Kershaw, M.J., Thornton, C.R., Schuster, M. et al. (2013) NADPH oxidases regulate septin-mediated cytoskeletal remodeling during plant infection by the rice blast fungus. *Proceedings of the National Academy of Sciences of the United States of America*, 110, 3179–3184.

Saunders, D.G., Dagdas, Y.F. & Talbot, N.J. (2010) Spatial uncoupling of mitosis and cytokinesis during appressorium-mediated plant infection by the rice blast fungus *Magnaporthe oryzae*. *The Plant Cell*, 22, 2417–2428.

Schultzhaus, Z., Quintanilla, L., Hilton, A. & Shaw, B.D. (2016) Live cell imaging of actin dynamics in the filamentous fungus *Aspergillus nidulans*. *Microscopy and Microanalysis*, 22, 264–274.

Schumacher, J. (2012) Tools for *Botrytis cinerea*: new expression vectors make the gray mold fungus more accessible to cell biology approaches. *Fungal Genetics and Biology*, 49, 483–497.

Skau, C.T., Courson, D.S., Bestul, A.J., Winkelman, J.D., Rock, R.S., Sirotkin, V. et al. (2011) Actin filament bundling by fimbrin is important for endocytosis, cytokinesis, and polarization in fission yeast. *Journal of Biological Chemistry*, 286, 26964–26977.

Skau, C.T. & Kovar, D.R. (2010) Fimbrin and tropomyosin competition regulates endocytosis and cytokinesis kinetics in fission yeast. *Current Biology*, 20, 1415–1422.

Su, H., Zhu, J., Cai, C., Pei, W., Wang, J., Dong, H. et al. (2012) FIMBRIN1 is involved in lily pollen tube growth by stabilizing the actin fringe. *The Plant Cell*, 24, 4539–4554.

Takeshita, N., Manck, R., Grün, N., de Vega, S.H. & Fischer, R. (2014) Interdependence of the actin and the microtubule cytoskeleton during fungal growth. *Current Opinion in Microbiology*, 20, 34–41.

Talbot, N.J. (2019) Appressoria. *Current Biology*, 29, R144–R146.

Tamura, K., Stecher, G. & Kumar, S. (2021) MEGA11: molecular evolutionary genetics analysis version 11. *Molecular Biology and Evolution*, 38, 3022–3027.

Upadhyay, S. & Shaw, B.D. (2008) The role of actin, fimbrin and endocytosis in growth of hyphae in *Aspergillus nidulans*. *Molecular Microbiology*, 68, 690–705.

Wang, J., Du, Y., Zhang, H., Zhou, C., Qi, Z., Zheng, X. et al. (2013) The actin-regulating kinase homologue MoArk1 plays a pleiotropic function in *Magnaporthe oryzae*. *Molecular Plant Pathology*, 14, 470–482.

Wang, C.L. & Shaw, B.D. (2016) F-actin localization dynamics during appressorium formation in *Colletotrichum graminicola*. *Mycologia*, 108, 506–514.

Wilson, R.A. & Talbot, N.J. (2009) Under pressure: investigating the biology of plant infection by *Magnaporthe oryzae*. *Nature Reviews Microbiology*, 7, 185–195.

Wu, Y., Yan, J., Zhang, R., Qu, X., Ren, S., Chen, N. et al. (2010) *Arabidopsis* FIMBRIN5, an actin bundling factor, is required for pollen germination and pollen tube growth. *The Plant Cell*, 22, 3745–3763.

Xiang, X. & Plamann, M. (2003) Cytoskeleton and motor proteins in filamentous fungi. *Current Opinion in Microbiology*, 6, 628–633.

Ye, J., Zheng, Y., Yan, A., Chen, N., Wang, Z., Huang, S. et al. (2009) *Arabidopsis* formin3 directs the formation of actin cables and polarized growth in pollen tubes. *The Plant Cell*, 21, 3868–3884.

Zhang, Z., Henderson, C., Perfect, E., Carver, T.L.W., Thomas, B.J., Skamnioti, P. et al. (2005) Of genes and genomes, needles and haystacks: *Blumeria graminis* and functionality. *Molecular Plant Pathology*, 6, 561–575.

Zheng, C., Zhang, W., Zhang, S., Yang, G., Tan, L. & Guo, M. (2021) Class I myosin mediated endocytosis and polarization growth is essential for pathogenicity of *Magnaporthe oryzae*. *Applied Microbiology and Biotechnology*, 105, 7395–7410.

SUPPORTING INFORMATION

Additional supporting information can be found online in the Supporting Information section at the end of this article.

How to cite this article: Zhang, Y., An, B., Wang, W., Zhang, B., He, C. & Luo, H. et al. (2022) Actin-bundling protein fimbrin regulates pathogenicity via organizing F-actin dynamics during appressorium development in *Colletotrichum gloeosporioides*. *Molecular Plant Pathology*, 23, 1472–1486. Available from: https://doi.org/10.1111/mpp.13242